SCIENCE CHINA
Information Sciences

• RESEARCH PAPER •

November 2016, Vol. 59 112210:1–112210:12
doi: 10.1007/s11432-015-0623-6

Conservation law-based air mass flow calculation in engine intake systems

Jixiang FAN[1,2], Yuhu WU[3], Akira OHATA[4] & Tielong SHEN[2]*

[1]*School of Physics and Electronic Engineering, Harbin Normal University, Harbin* 150025*, China;*
[2]*Department of Engineering and Applied Science, Sophia University, Tokyo* 102-8554*, Japan;*
[3]*School of Control Science and Engineering, Dalian University of Technology, Dalian* 116024*, China;*
[4]*Toyota Motor Corporation, Shizuoka* 410-1193*, Japan*

Received February 28, 2016; accepted May 18, 2016; published online October 10, 2016

Abstract In current engine controls, a number of control methods are based on the air charge estimation in engine intake systems. Since the derivative of the air mass flow through the throttle valve goes to infinity when the intake pressure is close to the upper stream pressure, the relatively large numerical error or oscillation occurs near the singularity point when using common algorithms. This paper develops an effective algorithm for calculating the air mass flow in engine intake systems. Utilizing the high-level model description (HLMD), the system is described by mass and energy conservation laws and therefor the singularity issue at the zero pressure-difference point is transformed into a singularity issue at the corresponding energy point. Then, the implicit midpoint rule, a special symplectic discrete method, is selected to integrate the energy and mass conservation system. The simulation results show that the numerical behaviour of the air mass flow is significantly improved at the singularity point by using the proposed algorithm. The experimental results also verify that the qualitative behaviour of the air mass flow calculated by the proposed algorithm is consistent with the actual physical system.

Keywords air mass flow, engine intake system, conservation law, singularity, numerical method

Citation Fan J X, Wu Y H, Ohata A, et al. Conservation law-based air mass flow calculation in engine intake systems. Sci China Inf Sci, 2016, 59(11): 112210, doi: 10.1007/s11432-015-0623-6

1 Introduction

In automotive engine control systems, some advanced control techniques such as spark advance control, air-fuel ratio control and variable valve timing control are effectively utilized to improve fuel economy and reduce emissions [1–4]. Since the majority of these control techniques depend on the estimation of air mass flows in the engine intake system, the accuracy of these estimated air mass flows significantly influences the control effect. However, the conventional formula [5] for air mass flow through the throttle valve, similarly the turbulent orifice flow, has an infinite derivative when the pressure difference across the throttle valve is zero. Therefore, it can be difficult to numerically calculate air mass flow when the pressure difference approaches zero.

When we use an automatic time-step adjustment algorithm to numerically integrate the system, this singularity can cause the time-step adjustment algorithm to drastically reduce the time step, which

* Corresponding author (email: tetu-sin@sophia.ac.jp)

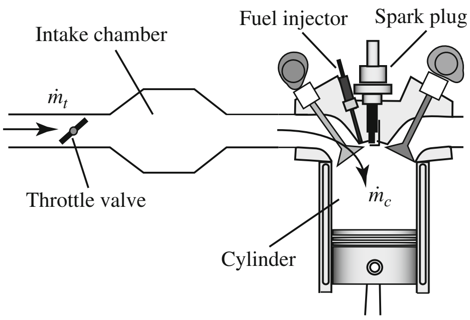

Figure 1 Schematic of the engine intake system.

inevitably results in either time-consuming calculation or failure. Alternatively, a stiff stable integration algorithm with a fixed time step, as developed by Bowns [6] and Krus [7], may ensure numerical stability, but the calculation accuracy depends on the time step chosen by the user, and sometimes numerical oscillation will appear around the singularity point. A simpler method for overcoming this problem is to remove the singularity from the formula by assuming laminar flow while the pressure difference is small [8]. Ellman and Piché [9] proposed a two-regime orifice formula in which an empirical polynomial laminar flow function is used for small pressure differences. Borutzky et al. [10] provided a different empirical flow formula to achieve the same purpose and realized a smooth transition from laminar to turbulent regimes. Although these two-regime orifice flow methods make the formula differentiable at the zero-pressure difference point and thus avoid the singularity, the existence of error is obvious and the error is directly relevant to the definition of the flow function in the laminar regime.

Consequently, the numerical calculation of air mass flow near the singularity point is one of the bottlenecks when estimating air charge in engine intake systems. In this work, we develop an algorithm to correctly describe the qualitative behaviour of air mass flow through the throttle valve in order to estimate the air charge of engine intake system. The air mass flow is derived using a novel high-level modeling (HLM) approach. Using high-level model description (HLMD), we can describe the system by mass and energy conservation laws. Therefore the singularity issue at the zero pressure-difference point can be transformed into a singularity issue at the corresponding energy point. The implicit midpoint rule, as a symplectic discrete method, which preserves the geometric properties of numerical flow of a differential equation [11], is utilized to discrete the target system. The simulation results are presented and compared with the results of several common numerical approaches and an experiment.

The rest of this paper is organized as follows: In Section 2, the physical model for air charge in engine intake systems is derived based on the HLMD. In Section 3, an algorithm for calculating the air mass flow is proposed. In Section 4, the simulation results based on the proposed algorithm are given and compared with the results of two fixed time-step algorithms, an automatic time-step adjustment algorithm and an experiment. Finally, the conclusion is drawn in Section 5.

2 HLMD of air mass flow in engine intake systems

The HLM approach provides a framework for rapidly developing physics-based models and is being applied to vehicle systems [12–15]. The main advantages of this approach are that it can describe a multi-domain physical system using a simple domain-neutral methodology based on considered conservation laws and constraints, and it can clearly show the design intention at the physical level so that the model can be efficiently understood and peer-reviewed from the physical perspective. In this section, a physical model of the air mass flow in engine intake systems is derived based on the HLM approach.

Figure 1 shows a schematic of the engine intake system under consideration. In this figure, only one cylinder is drawn although a six-cylinder engine is modeled in this study. The intake air is drawn from the atmosphere to the intake chamber through the throttle valve, and the gas flows out from the cylinders to the atmosphere through the exhaust valve.

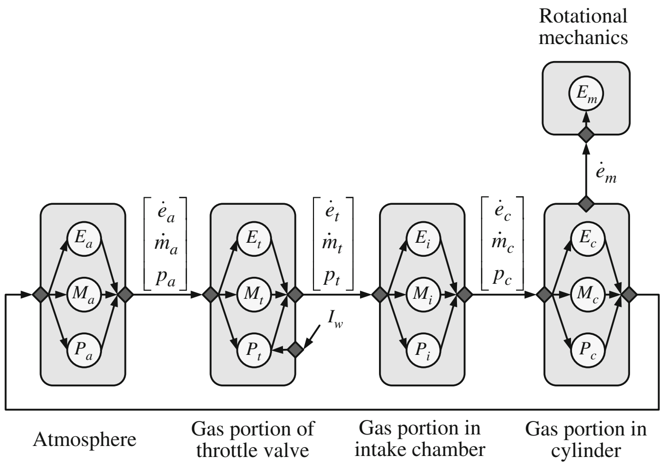

Figure 2 HLMD of the air portion in the engine intake system.

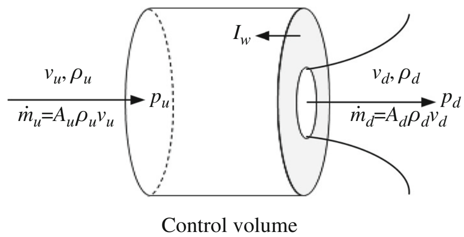

Figure 3 Flow model through the throttle valve.

Figure 2 shows the HLMD of the air portion in the engine intake system, which consists of five components, i.e., the atmosphere, the gas portions of the throttle valve, the intake chamber, the cylinder and the rotational portion of the engine. The rectangular blocks with rounded corners denote the corresponding components, the circles denote the storage of conserved quantities, the arrows denote the flows of the conserved quantities and their directions indicate the mathematical sign convention. The capital E_* , M_* and P_* denote the amounts of energy, mass and momentum, respectively, and the small $\dot{e}_*$ and $\dot{m}_*$ denote the energy and mass flows, respectively. p_* denotes the momentum flow density, which represents the momentum flow unit area. Since the momentum flow density is represented in units of Newton per square metre, it is thus equivalent to pressure in thermodynamics. The suffixes a, t, i, c and m denote the sources of the flows, i.e., the atmosphere, the throttle valve, the intake chamber, the cylinder and the engine rotational portion, respectively. I_w indicates the momentum flow from the wall that corresponds to the force acting on the surface of the throttle valve. In this study, the quasi-steady state is supposed when the air flows through the throttle valve and the velocities of gas in the atmosphere, the intake chamber and the cylinder are neglected. Thus $P_a = 0$, $P_i = 0$ and $P_c = 0$.

In order to describe the behaviour of gas flowing through the throttle valve, the control volume method [16] is utilized. The gas portion of throttle valve corresponds to the control volume shown in Figure 3. where v_u, ρ_u , $\dot{m}_u$ and p_u denote the gas velocity, density, mass flow and momentum flow density at the inlet side of the control volume, respectively, and v_d, ρ_d, $\dot{m}_d$ and p_d denote the corresponding physical parameters at the outlet side of the control volume, respectively. A_u and A_d denote the areas of the inlet and outlet, respectively. The total momentum flow from the wall can be approximately calculated by

$$I_w = \int_{A_d}^{A_u} p_u \, \mathrm{d}A \approx (A_u - A_d)\, p_u. \tag{1}$$

In view of the assumption of quasi-steady state flow, the mass, energy and momentum conservation laws at the throttle valve can be expressed as

$$A_u \, \rho_u \, v_u = A_d \, \rho_d \, v_d, \tag{2}$$

$$A_u \, \rho_u \, v_u \left(\frac{f+2}{2} \frac{p_u}{\rho_u} + \frac{1}{2} v_u^2 \right) = A_d \, \rho_d \, v_d \left(\frac{f+2}{2} \frac{p_d}{\rho_d} + \frac{1}{2} v_d^2 \right), \tag{3}$$

$$A_u \, p_u + A_u \, \rho_u \, v_u^2 - (A_u - A_d)\, p_u = A_d \, p_d + A_d \, \rho_d \, v_d^2, \tag{4}$$

where f is the degree of freedom of air.

Because the inlet is the atmosphere, its area A_u thus can be viewed as infinite. Moreover, considering the air mass flow $\dot{m}_u$ and density ρ_u must take finite values, thus from equation $\dot{m}_u = A_u \, \rho_u \, v_u$ we can deduce that the gas velocity v_u should tend to zero.

Substituting (2) into (3) and considering $v_u = 0$, the energy and momentum conservation laws (3) and (4), respectively, can be simply rewritten as

$$\frac{f+2}{2}\frac{p_u}{\rho_u} = \frac{f+2}{2}\frac{p_d}{\rho_d} + \frac{1}{2}v_d^2, \tag{5}$$

$$p_u = p_d + \rho_d\, v_d^2. \tag{6}$$

Using the momentum conversation law (6), the air mass flow at the outlet side of the control volume is thus

$$\dot{m}_d = A_d \cdot \rho_d \cdot v_d = A_d \cdot \sqrt{\rho_d\,(p_u - p_d)}. \tag{7}$$

Eliminating the gas velocity v_d in (5) and (6), we obtain the gas density at the outlet side of the control volume as

$$\rho_d = \frac{(f+1)\,p_d + p_u}{(f+2)\,p_u}\rho_u. \tag{8}$$

Then, substituting (8) into (7), we can calculate the mass flow $\dot{m}_d$ as follows

$$\begin{aligned}\dot{m}_d &= A_d\sqrt{\frac{(f+1)p_d + p_u}{(f+2)p_u}\rho_u\,(p_u - p_d)}\\ &= A_d\sqrt{(f+1)\,p_u\rho_u}\cdot\sqrt{\frac{1}{f+2}\left(\left(\frac{f+2}{2\,(f+1)}\right)^2 - \left(\frac{f}{2\,(f+1)} - \frac{p_d}{p_u}\right)^2\right)}.\end{aligned} \tag{9}$$

Taking the sonic condition into account, namely, the sonic speed expressed by the following formula is the highest velocity of the gas flow [15],

$$v_s = \sqrt{\frac{f+2}{f}\frac{p_d}{\rho_d}}, \tag{10}$$

one can obtain the following critical pressure $p_{\rm cr}$ by substituting (10) into (6).

$$p_{\rm cr} = \frac{f}{2(f+1)}p_u. \tag{11}$$

Therefore, during the intake process, p_d should be replaced by p_i when $p_i > p_{\rm cr}$ and by $p_{\rm cr}$ when $p_i \leqslant p_{\rm cr}$ in view of the sonic condition and the assumption that the effect of p_i does not transfer to the upper stream.

With the sonic condition, and considering that the inverse behaviour occurs when the gas pressure in the intake chamber is greater than the atmospheric pressure, the air mass flow through the throttle valve can be expressed by the following piecewise functions.

$$\dot{m}_t = \begin{cases} A\sqrt{(f+1)\,p_a\rho_a}\cdot\Phi\left(\dfrac{p_i}{p_a}\right), & p_a > p_i,\\ A\sqrt{(f+1)\,p_i\rho_i}\cdot\Phi\left(\dfrac{p_a}{p_i}\right), & p_a \leqslant p_i,\end{cases} \tag{12}$$

with

$$\Phi(x) = \begin{cases} \operatorname{sign}(1-x)\sqrt{\dfrac{1}{f+2}\left(\left(\dfrac{f+2}{2(f+1)}\right)^2 - \left(\dfrac{f}{2(f+1)} - x\right)^2\right)}, & x > \dfrac{f}{2(f+1)},\\ \operatorname{sign}(1-x)\sqrt{\dfrac{f+2}{(2(f+1))^2}}, & x \leqslant \dfrac{f}{2(f+1)},\end{cases} \tag{13}$$

where A is the throttle valve opening area, which varies with the change in the throttle angle θ based on a simple geometric consideration as

$$A\,(\theta) = \pi\cdot\left(\frac{D}{2}\right)^2\cdot(1-\cos\theta)\,, \tag{14}$$

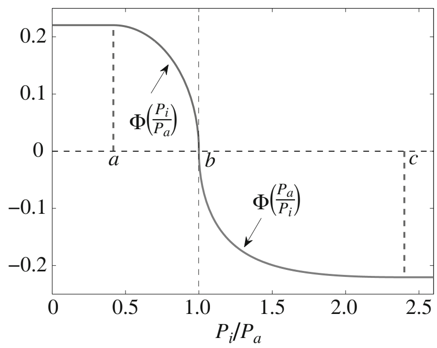

Figure 4 Nonlinear function $\Phi(\cdot)$.

where D is the diameter of the throttle bore.

In contrast to the conventional formula [5] for air mass flow through the throttle valve, which is derived by the thermodynamic relationship for isentropic expansion, the proposed formula is derived by the energy and momentum conservation laws, which is the distinguishing characteristic of the HLM approach.

During the intake stroke, considering the assumption that the heat transfer from the cylinder wall is neglected, the composition of the gas in the cylinder is constant. In addition, the cylinder pressure is equal to the atmospheric pressure at the beginning of the intake stroke and the cylinder pressure is equal to the intake chamber pressure during the intake stroke. Thus in one intake stroke, the energy change ΔE_c in one cylinder can be expressed as

$$\Delta E_c = \frac{f}{2}\left(P_i V_b - P_a V_t\right) + P_i\left(V_b - V_t\right). \tag{15}$$

On the right side of (15), the first and second terms represent the variation in the thermal energy and the pressure volume work, respectively. V_b is the cylinder volume at the bottom dead centre (BDC) and V_t is that one at the top dead centre (TDC).

For a six-cylinder/four-stroke engine, the increase in energy in the six cylinders per second is therefore $\Delta E_c \cdot \omega/20$, where ω is the engine rotational speed.

Based on the energy conservation law, these energy increases in the cylinders are equal to the energy of the air simultaneously induced from the intake chamber into the cylinders and can be formalized as

$$\frac{f+2}{2}\dot{m}_c R_g T_i = \frac{\omega}{20}\cdot\frac{f}{2}\left(P_i V_b - P_a V_t\right) + P_i\left(V_b - V_t\right), \tag{16}$$

where R_g is the gas constant of the air and T_i is the gas temperature in the intake chamber. Therefore, the air mass flow induced into the cylinders can be obtained as

$$\dot{m}_c = \frac{\omega}{30}\cdot\frac{\frac{f+2}{2}\,p_i\,V_b - (\frac{f}{2}\,p_a + p_i)\,V_t}{\frac{f+2}{2}\,R_g\,T_i}. \tag{17}$$

Eqs. (12) and (17) describe the entire air charge in the engine intake system. In (12), it is noted that Φ is the square root function of the pressure ratio. Moreover, the derivative of Φ with respect to the pressure ratio is infinite at the point where the pressure ratio is one. This can be illustrated in the curve of the nonlinear function Φ, as shown in Figure 4. In this figure, the left side of point a and the right side of point c are the regions of critical pressure where the air flow reaches the sonic condition. Point b is the singularity point where the derivative of Φ is infinite. Therefore, there is the numerical difficulty at this singularity point. In addition, since the air mass flow $\dot{m}_f$ is calculated by the piecewise function based on the intake chamber pressure, as expressed by (12), this piecewise function results in frequent role switching between the upper and down streams when the pressure ratio is close to one, so oscillation will occur and persist. In order to overcome these problems, in the next section we propose an algorithm for numerically calculating air mass flow.

3 Algorithm for calculating air mass flow

In mechanics, symplectic integrators are a kind of effectively numerical integration method, which can preserve the geometric properties of the numerical flow of a differential equation and thus can correctly describe the qualitative behaviour of a target system [11, 17, 18]. In general, symplectic integrators own implicit or semi-implicit form. The implicit midpoint rule, as typical one, may achieve an effective trade-off between computational efficiency and accuracy. Therefore, in this study, we adopt the implicit midpoint rule to discretize the system.

According to the presented HLMD of the engine intake system shown in Figure 2, in the intake chamber, the air charge obeys mass and energy conservation laws, which can be expressed by

$$\frac{\mathrm{d}M_i}{\mathrm{d}t} = \dot{m}_t - \dot{m}_c, \tag{18}$$

$$\frac{\mathrm{d}E_i}{\mathrm{d}t} = \frac{f+2}{2} R_g T_u \dot{m}_t - \frac{f+2}{2} R_g T_i \dot{m}_c, \tag{19}$$

where T_u is the gas temperature at the upper stream of the throttle valve. When the air flows from the atmosphere to the intake chamber, T_u represents the atmospheric temperature T_a. In contrast, T_u represents the temperature of the gas in the intake chamber T_i. Thus, T_u can be denoted by the following piecewise function.

$$T_u = \begin{cases} T_a, & p_a > p_i, \\ T_i, & p_a \leqslant p_i. \end{cases} \tag{20}$$

Subsequently, only the amounts of energy and mass in the intake chamber are mentioned, thus the suffix i in M_i and E_i is omitted to simplify the notation.

The amount of mass in the intake chamber can be written as

$$M = \rho_i V_i, \tag{21}$$

where V_i denotes the volume of the intake chamber, and ρ_i denotes the density of the gas in the intake chamber, which can be calculated based on the intake chamber pressure p_i and temperature T_i as

$$\rho_i = \frac{p_i}{R_g T_i}. \tag{22}$$

The amount of energy in the intake chamber can be written as

$$E = \frac{f}{2} p_i V_i. \tag{23}$$

According to (12) and (17), the air mass flow $\dot{m}_t$ is the function of p_i and ρ_i, and the air mass flow $\dot{m}_c$ is the function of p_i and T_i. Moreover, according to (21)–(23), the p_i , ρ_i and T_i can be expressed as the function of intake chamber mass M and energy E. Consequently, the mass and energy conservation laws, described by (18) and (19), can be rewritten as

$$\frac{\mathrm{d}M}{\mathrm{d}t} = f_1(M, E), \tag{24}$$

$$\frac{\mathrm{d}E}{\mathrm{d}t} = f_2(M, E). \tag{25}$$

These two ordinary differential equations describe the changes in the mass and energy of the gas in the intake chamber caused by the air flows. Thus, if we discretize the system represented by (24) and (25), the numerical solutions for M and E can be obtained, and then the air flows $\dot{m}_t$ and $\dot{m}_c$ can be calculated according to (12) and (17) by replacing p_i, ρ_i and T_i with the corresponding functions of M and E.

In order to apply the implicit midpoint rule to discretize the system, we rewrite the piecewise $\dot{m}_t$ and T_u, respectively, as uniform forms using the sign function, i.e., (26) and (27). Note that in these two equations, p_i, ρ_i and T_i are replaced by the corresponding functions of M and E.

$$\begin{aligned}\dot{m}_t =& \operatorname{sign}(p_a-p_i)A\sqrt{(f+1)\left(\frac{1-\operatorname{sign}(p_a-p_i)}{2}p_i\rho_i+\frac{1+\operatorname{sign}(p_a-p_i)}{2}p_a\rho_a\right)}\\ &\cdot\left(\frac{1}{f+2}\left(\left(\frac{f+2}{2(f+1)}\right)^2-\left(\frac{f}{2(f+1)}-\left(\frac{1+\operatorname{sign}[(\frac{p_i}{p_a})^{\operatorname{sign}(p_a-p_i)}-\frac{f}{2(f+1)}]}{2}\left(\frac{p_i}{p_a}\right)^{\operatorname{sign}(p_a-p_i)}\right.\right.\right.\right.\\ &\left.\left.\left.\left.+\frac{1-\operatorname{sign}[(\frac{p_i}{p_a})^{\operatorname{sign}(p_a-p_i)}-\frac{f}{2(f+1)}]}{2}\frac{f}{2(f+1)}\right)\right)^2\right)\right)^{\frac{1}{2}},\end{aligned} \tag{26}$$

$$T_u = \frac{1+\operatorname{sign}(p_a-p_i)}{2}T_a+\frac{1-\operatorname{sign}(p_a-p_i)}{2}T_i. \tag{27}$$

Next we discrete the differential equations of energy and mass by the implicit midpoint rule with fixed time step h as

$$M_{k+1} = M_k + hf_1\left(\frac{M_k+M_{k+1}}{2},\frac{E_k+E_{k+1}}{2}\right), \tag{28}$$

$$E_{k+1} = E_k + hf_2\left(\frac{M_k+M_{k+1}}{2},\frac{E_k+E_{k+1}}{2}\right). \tag{29}$$

and obtain the corresponding discrete system, as shown by (30) and (31).

$$\begin{aligned}M_{k+1} =& M_k + h\cdot\operatorname{sign}\left(p_a-\frac{E_k+E_{k+1}}{f\cdot V_i}\right)A\cdot\left(\frac{f+1}{f+2}\left(\frac{1-\operatorname{sign}(p_a-\frac{E_k+E_{k+1}}{f\cdot V_i})}{2}\cdot\frac{E_k+E_{k+1}}{f\cdot V_i}\right.\right.\\ &\left.\left.\cdot\frac{M_k+M_{k+1}}{2V_i}+\frac{1+\operatorname{sign}(p_a-\frac{E_k+E_{k+1}}{f\cdot V_i})}{2}p_a\rho_a\right)\right)^{\frac{1}{2}}\cdot\left(\left(\frac{f+2}{2(f+1)}\right)^2-\left(\frac{f}{2(f+1)}\right.\right.\\ &-\left(\frac{1+\operatorname{sign}[(\frac{E_k+E_{k+1}}{p_a\cdot f\cdot V_i})^{\operatorname{sign}(p_a-\frac{E_k+E_{k+1}}{f\cdot V_i})}-\frac{f}{2(f+1)}]}{2}\cdot\left(\frac{E_k+E_{k+1}}{p_a\cdot f\cdot V_i}\right)^{\operatorname{sign}\left(p_a-\frac{E_k+E_{k+1}}{f\cdot V_i}\right)}\right.\\ &\left.\left.\left.+\frac{1-\operatorname{sign}[(\frac{E_k+E_{k+1}}{p_a\cdot f\cdot V_i})^{\operatorname{sign}(p_a-\frac{E_k+E_{k+1}}{f\cdot V_i})}-\frac{f}{2(f+1)}]}{2}\cdot\frac{f}{2(f+1)}\right)\right)^2\right)^{\frac{1}{2}}\\ &-h\cdot\frac{\omega}{30}\frac{\frac{f+2}{2}\cdot\frac{E_k+E_{k+1}}{f\cdot V_i}\cdot V_b-(\frac{f}{2}p_a+\frac{E_k+E_{k+1}}{f\cdot V_i})V_t}{\frac{f+2}{f}\frac{E_k+E_{K+1}}{M_k+M_{k+1}}},\end{aligned} \tag{30}$$

$$\begin{aligned}E_{k+1} =& E_k + h\left(\frac{f+2}{2}R_g\left(\frac{1+\operatorname{sign}(p_a-\frac{E_k+E_{k+1}}{f\cdot V_i})}{2}T_a+\frac{1-\operatorname{sign}(p_a-\frac{E_k+E_{k+1}}{f\cdot V_i})}{f\cdot R_g}\frac{E_k+E_{K+1}}{M_k+M_{k+1}}\right)\right)\\ &\cdot\operatorname{sign}\left(p_a-\frac{E_k+E_{k+1}}{f\cdot V_i}\right)A\cdot\left(\frac{f+1}{f+2}\left(\frac{1-\operatorname{sign}(p_a-\frac{E_k+E_{k+1}}{f\cdot V_i})}{2}\cdot\frac{E_k+E_{k+1}}{f\cdot V_i}\cdot\frac{M_k+M_{k+1}}{2V_i}\right.\right.\\ &\left.\left.+\frac{1+\operatorname{sign}(p_a-\frac{E_k+E_{k+1}}{f\cdot V_i})}{2}p_a\rho_a\right)\right)^{\frac{1}{2}}\cdot\left(\left(\frac{f+2}{2(f+1)}\right)^2-\left(\frac{f}{2(f+1)}\right.\right.\\ &-\left(\frac{1+\operatorname{sign}((\frac{E_k+E_{k+1}}{p_a\cdot f\cdot V_i})^{\operatorname{sign}(p_a-\frac{E_k+E_{k+1}}{f\cdot V_i})}-\frac{f}{2(f+1)})}{2}\cdot\left(\frac{E_k+E_{k+1}}{p_a\cdot f\cdot V_i}\right)^{\operatorname{sign}\left(p_a-\frac{E_k+E_{k+1}}{f\cdot V_i}\right)}\right.\end{aligned}$$

Table 1 Model parameters used in simulation

Parameter	Value
Atmospheric pressure P_a	1.0132×10^5 Pa
Atmospheric temperature T_a	298.15 K
Air density ρ_a	1.18 kg/m^3
Gas constant of air R_g	287.1 J/kg·K
Degree of freedom of air f	5
Diameter of throttle bore D	0.094 m
Intake chamber volume V_i	0.0054 m^3
Cylinder volume at BDC V_c	6.2934×10^{-4} m^3
Cylinder volume at TDC V_t	5.3333×10^{-5} m^3
Engine speed ω	1000 rpm

$$
\left.\left.\left.\left. + \frac{1 - \mathrm{sign}\left(\left(\frac{E_k+E_{k+1}}{p_a \cdot f \cdot V_i}\right)^{\mathrm{sign}\left(p_a - \frac{E_k+E_{k+1}}{f \cdot V_i}\right)} - \frac{f}{2(f+1)}\right)}{2} \cdot \frac{f}{2(f+1)} \right)\right)^2 \right)^{\frac{1}{2}}
$$

$$
- h \cdot \frac{\omega}{30} \left(\frac{f+2}{2} \cdot \frac{E_k + E_{k+1}}{f \cdot V_i} \cdot V_b - \left(\frac{f}{2} p_a + \frac{E_k + E_{k+1}}{f \cdot V_i} \right) V_t \right). \tag{31}
$$

By solving this implicit discrete system, we can obtain M_k and E_k $(k = 1, \ldots, N)$ and we also can calculate the corresponding air mass flows $\dot{m}_t$ and $\dot{m}_c$.

We can summarize, the algorithm for calculating the air mass flow of engine intake systems as follows:

- Express p_i, ρ_i and T_i as functions of M and E, i.e., (21)–(23);
- Rewrite piecewise $\dot{m}_t$ and T_u into uniform forms, i.e., (26) and (27), by utilizing the sign function, respectively;
- Replace p_i, ρ_i and T_i in (26), (27) and (17), respectively, by M and E according to the functions presented in the first step;
- Discretize the mass and energy conservation laws, (18) and (19), by the implicit midpoint rule to obtain the discrete system, i.e., (30) and (31);
- Solve the discrete system to obtain M_k and E_k $(k = 1, \ldots, N)$ and then calculate the corresponding air mass flows $\dot{m}_t$ and $\dot{m}_c$ according to (26) and (17) with the third step.

4 Results and comparison

In this section, some simulations and an experiment are performed to verify the validity of the proposed algorithm. Using the algorithm presented in Section 3, the simulations are performed in MATLAB. For comparison, two common discrete methods with fixed step, i.e., explicit Euler method and 4 order Runge Kutta method, and a discrete method with variable step, i.e., 4–5 order Dormand/Prince Runge Kutta method, are used to solve the same problem. For the fixed-step solvers, the sampling time is selected as 1ms, and for the variable-step solver, the relative tolerance is selected as 10^{-3}. The model parameters are listed in Table 1. The selected parameter values are consistent with those in the experimental environment and in the actual Toyota V6 engine used in the experiment.

To observe the numerical behaviour of the air flows through the throttle valve and particularly in the situation in which the pressure ratio across the throttle valve tends to one, the throttle angle is specified to vary according to the rule shown in Figure 5(a). For comparison, the same throttle-angle change rule is used in the various numerical methods and in the experiment. Figure 5 (b) to (e) show the air flows through the throttle valve and induced into the cylinder and the intake chamber pressure, using the explicit Euler (EE), 4 order Runge Kutta (RK4), 4–5 order Dormand/Prince Runge Kutta (DPRK54) and the proposed implicit midpoint (IM) methods, respectively.

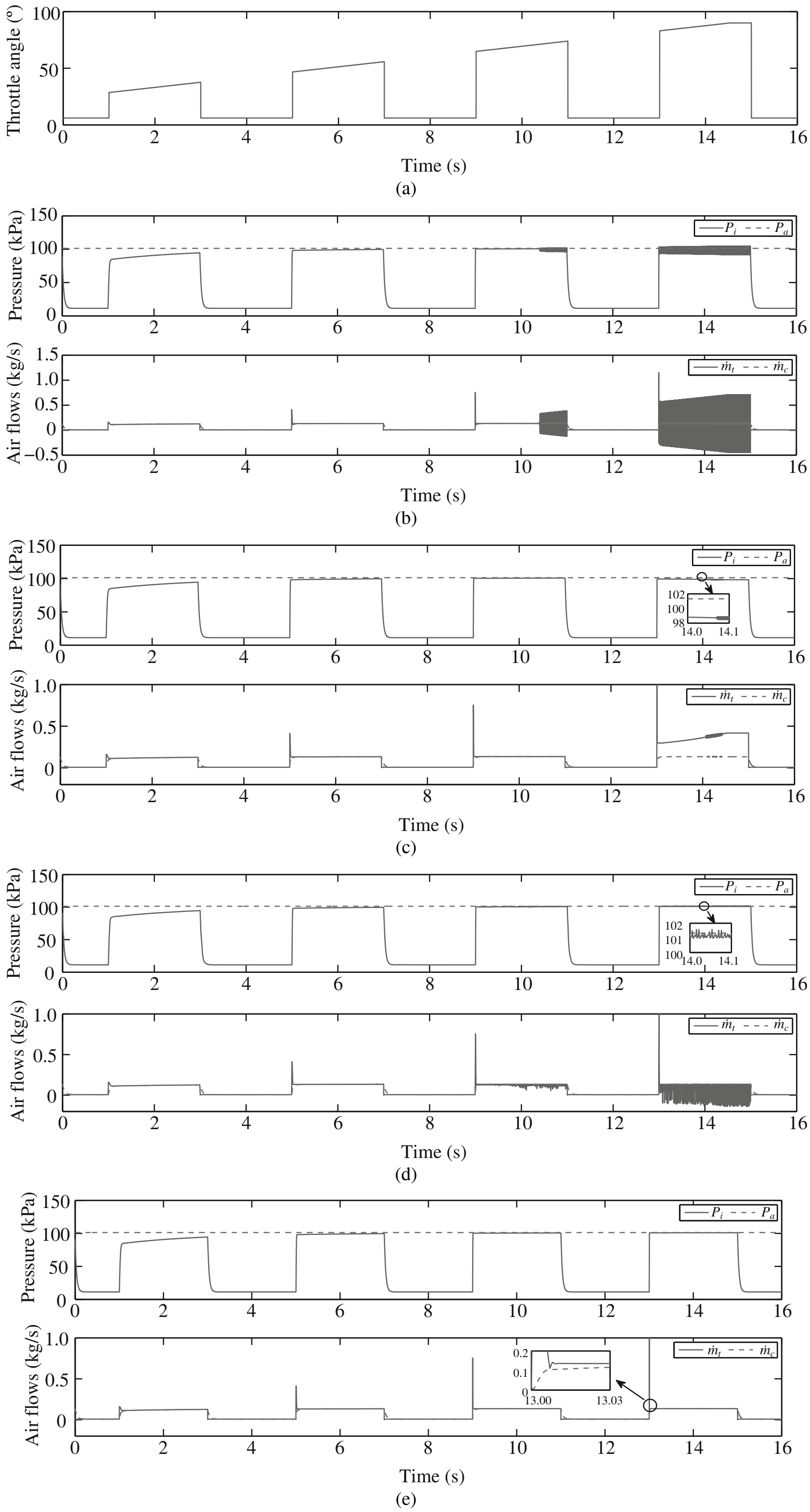

Figure 5 Throttle angle, air mass flows and pressures. (a) Throttle angle; (b) explicit Euler method; (c) 4 order Runge Kutta method; (d) 4 and 5 orders Dormand/Prince Runge Kutta method; (e) implicit midpoint method.

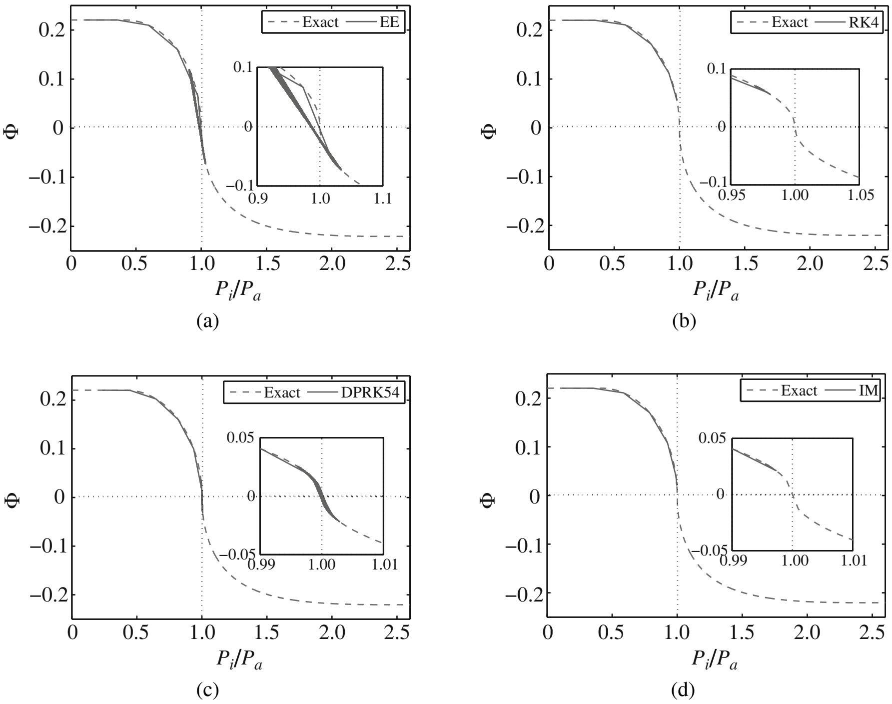

Figure 6 Simulation results of nonlinear function Φ at 12 to 15 s. (a) Explicit Euler; (b) 4 order Runge Kutta; (c) 4–5 order Dormand/Prince Runge Kutta; (d) implicit midpoint.

In the explicit Euler method, it is observed from Figure 5(b) that oscillations in the air mass flow $\dot{m}_t$ and intake chamber pressure P_i occur when the pressure difference on both sides of the throttle valve goes to zero and do so clearly at 10.5 to 11 and again at 13 to 15 seconds. The reason for this phenomenon is that the explicit Euler method calculates the air mass flow using the piecewise function based on the intake chamber pressure. Therefore, near the pressure balance point, i.e., where the pressure difference on both sides of the throttle valve is close to zero, this fixed-step algorithm leads to the frequent role transformation of the upper and down streams, which results in the oscillation.

Notes the fact that after the throttle is sufficiently opened, the air pressure between the atmosphere and intake chamber gradually balances, and at that time, the air mass flow induced into cylinder should be equal to the air mass flow through the throttle valve, i.e., $\dot{m}_c = \dot{m}_t$. However, in the RK4 method, although no oscillation occurs in the air mass flow $\dot{m}_t$ and intake chamber pressure P_i, a steady-state error in the air mass flow $\dot{m}_t$ is apparent, as shown in Figure 5(c).

When using the DPRK54 method, oscillation also occurs in the air flow $\dot{m}_t$ and intake chamber pressure P_i when the pressure difference on both sides of the throttle valve goes to zero (see Figure 5(d)), despite the fact that the amplitude of the oscillation is relatively small.

From the simulation results using the proposed midpoint rule, as shown in Figure 5(e), it can be observed that oscillation in the air mass flow $\dot{m}_t$ occurs only at the initial stage of the throttle opening, and the amplitude of the oscillation rapidly reduces. The steady-state error in the air mass flow $\dot{m}_t$ is dramatically smaller compared with that of the RK4 method.

Figure 6 illustrates the nonlinear function Φ using four different discrete methods during the time region from 12 to 15 seconds. In this figure, the four subgraphs show the curves of function Φ near the singularity points using different discrete methods. From this figure, it can be observed that when the pressure ratio is not near to the singularity point, the curves of function Φ calculated by the different numerical methods approximate the exact curves. However, when the pressure ratio is close to one, continuous oscillation occurs in the results of the explicit Euler and DPRK54 methods, as shown in Figure 6 (a) and (c). Therefore, these two discrete methods cannot correctly describe the behaviour of the proposed system near the singularity point. Although oscillation does not occur when using the RK4

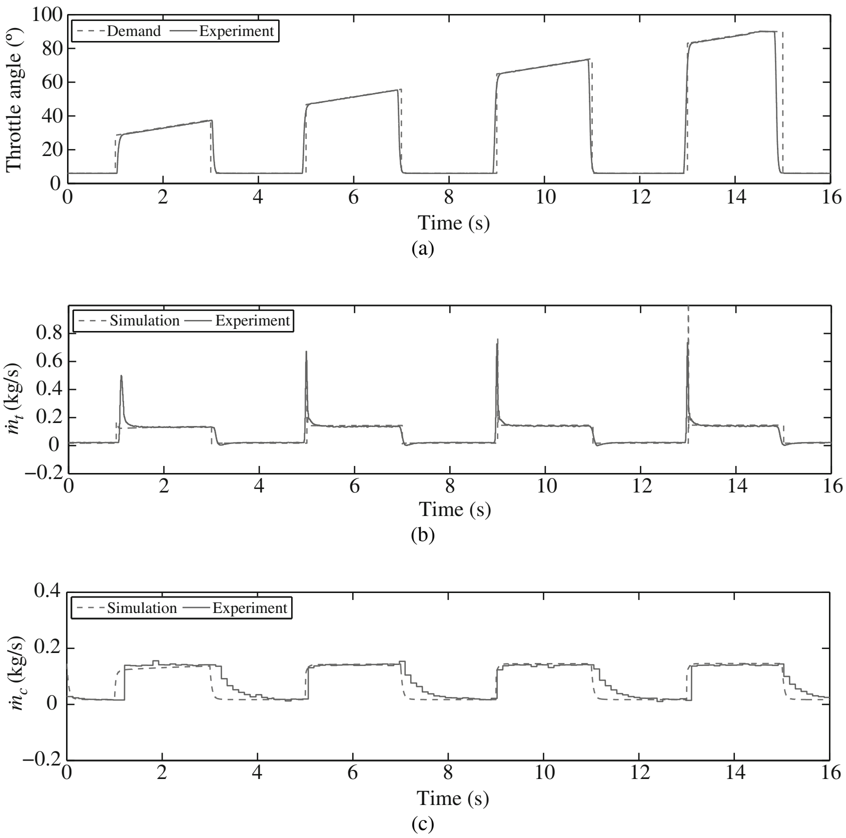

Figure 7 Simulation and experimental results on throttle angle and air mass flows. (a) Throttle angle; (b) air mass flow $\dot{m}_t$; (c) air mass flow $\dot{m}_c$.

method, as shown in Figure 6(b), the error caused by this numerical method is very large. When using the implicit midpoint method (see Figure 6(d)), oscillations occur several times only when the pressure ratio goes to one, and the error is smaller than that of the RK4 method.

To verify that the qualitative behaviour of the air mass flow calculated by the proposed algorithm is consistent with the actual physical system, the experiment is performed on a Toyota V6 engine test bench. The experimental results are shown in Figure 7. As shown in this figure, the throttle angle of the actual engine can change following the throttle angle demand (see Figure 7(a)). During the change of throttle angle, the air mass flow in the experiment did not generate oscillation. This physical behaviour of the air mass flow is consistent with the simulation results obtained by the proposed algorithm (see Figure 7 (b) and (c)). Therefore, the proposed algorithm for numerically calculating air mass flow can correctly describe the qualitative behaviour of air mass flow in actual engine intake systems.

From these simulation and experimental results, we have illustrated that the proposed numerical method has an advantage over the common numerical methods used to calculate air mass flow because it can correctly describe the qualitative behaviour of the air charge system.

5 Conclusion

In this paper, an algorithm is proposed for calculating the air mass flows in engine intake systems. This algorithm can correctly describe the qualitative behaviour of air mass flow through the throttle valve and in particular at the singularity point where the pressure difference across the throttle valve is zero. In this algorithm, the physical model of air mass flows is built based on the HLM method. Moreover, the implicit midpoint rule is utilized to discretize the essential conservation laws in order to numerically calculate the air mass flow. The simulation results show the oscillation that is generally caused by the traditional explicit fixed-step approach has disappeared and that the steady-state error is smaller. The experimental results verify the validity of the proposed algorithm. In fact, this algorithm is also suitable for the conventional air mass flow model described by the piecewise function if the conventional model is modified from the mass and energy conservation perspective. Applying this algorithm to the conventional model will be our further work.

Conflict of interest The authors declare that they have no conflict of interest.

References

1 Saraswati S, Agarwal P K, Chand S. Neural networks and fuzzy logic-based spark advance control of SI engines. Expert Syst Appl, 2011, 38: 6916–6925
2 Yang J, Shen T, Jiao X. Model-based stochastic optimal air-fuel ratio control with residual gas fraction of spark ignition engines. IEEE Trans Contr Syst Technol, 2014, 22: 896–910
3 Xie H, Song K, He Y. A hybrid disturbance rejection control solution for variable valve timing system of gasoline engines. ISA Trans, 2014, 53: 889–898
4 Wu Y, Kumar M, Shen T. A stochastic logical system approach to model and optimal control of cyclic variation of residual gas fraction in combustion engines. Appl Therm Eng, 2016, 93: 251–259
5 Guzzella L, Onder C. Introduction to Modeling and Control of Internal Combustion Engine Systems. Berlin: Springer Science & Business Media, 2009. 30–39
6 Bowns D E, Tomlinson S P, Dorey R E. Computer simulation techniques for the dynamic performance assessment of fuild power system. In: Proceedings of the 7th International Fluid Power Symposium, Bath, 1986. 81–88
7 Krus P. The simulation of fluid power system with complex load dynamics. Int J Model Simul, 1986, 6: 52–57
8 Ellman A, Vilenius M J. Methods for Simulating Steady-State and Dynamic Behavior of Two-Way Cartridge Valve Circuits. SAE Technical Paper 901584. 1990
9 Ellman A, Piché R. A two regime orifice flow formula for numerical simulation. J Dyn Sys Meas Control, 1999, 121: 721–724
10 Borutzky W, Barnard B, Thoma J. An orifice flow model for laminar and turbulent conditions. Simul Model Pract Theory, 2002, 10: 141–152
11 Hairer E, Lubich C, Wanner G. Geometric Numerical Integration: Structure-preserving Algorithms for Ordinary Differential Equations. Berlin: Springer Science & Business Media, 2006. 204–211
12 Ito H, Yohata H, Kako J, et al. Development of High Level Modeling Method for Rapid Modeling Process. SAE Technical Paper 2013-01-0244. 2013
13 Kako J, Sata K, Ohata A, et al. Effect of transient residual gas fraction for gasoline engines. In: Proceedings of the 32nd Chinese Control Conference (CCC), Xi'an, 2013. 7762–7767
14 Edelberg K, Hedrick J K. A high level approach to mean value modeling of an automotive engine during cold-start. In: Proceedings of 2014 American Control Conference (ACC), Portland, 2014. 3165–3170
15 Ohata A. Physical turbocharger model on high level model descrition (HLMD). In: Proceedings of the 7th IFAC Symposium on Advances in Automotive Control, Tokyo, 2013. 289–294
16 Eriksson L. Modeling and control of turbocharged SI and DI engines. Oil Gas Sci Technol, 2007, 62: 523–538
17 Marsden J E, West M. Discrete mechanics and variational integrators. Acta Numer, 2001, 10: 357–514
18 Chyba M, Hairer E, Vilmart G. The role of symplectic integrators in optimal control. Optim Contr Appl Methods, 2009, 30: 367–382